PLOS ONE

RESEARCH ARTICLE

# Estimation of leaf water content from hyperspectral data of different plant species by using three new spectral absorption indices

**Hong Li**[1,2], **Wunian Yang**[1]*, **Junjie Lei**[1], **Jinxing She**[1], **Xiangshan Zhou**[1]

**1** College of Earth Science, Chengdu University of Technology, Chengdu, China, **2** Geology and Surveying Engineering School, Chongqing Vocational Institute of Engineering, Chongqing, China

* ywn@cdut.edu.cn





**Citation:** Li H, Yang W, Lei J, She J, Zhou X (2021) Estimation of leaf water content from hyperspectral data of different plant species by using three new spectral absorption indices. PLoS ONE 16(3): e0249351. https://doi.org/10.1371/journal.pone.0249351

**Editor:** Claudionor Ribeiro da Silva, Universidade Federal de Uberlandia, BRAZIL

**Received:** December 10, 2020

**Accepted:** March 16, 2021

**Published:** March 30, 2021



**Data Availability Statement:** All relevant data are within the manuscript and its Supporting information files.

**Funding:** This study was financially supported by the National Natural Science Foundation of China (Grant No. 41671432) and Science and Technology Research Project of Chongqing Education Commission (Grant No. KJQN201803402).

**Competing interests:** The authors have declared that no competing interests exist.

## Abstract

The leaf equivalent water thickness (EWT, g $cm^{-2}$) and fuel moisture content (FMC, %) are key variables in ecological and environmental monitoring. Although a variety of hyperspectral vegetation indices have been developed to estimate the leaf EWT and FMC, most of these indices are defined considered two or three specific bands for a specific plant species, which limits their applicability. In this study, we proposed three new spectral absorption indices ($SAI_{970}$, $SAI_{1200}$, and $SAI_{1660}$) for various plant types by considering the symmetry of the spectral absorption at 970 nm, 1200 nm and 1660 nm and spectral heterogeneity of different leaves. The indices were calculated considering the absorption peak and shoulder bands of each leaf instead of the same specific bands for all leaves. A pooled dataset of three tree species (camphor (VX), capricorn (VJ), and red-leaf plum (VL)) was used to test the performance of the SAIs in terms of the leaf EWT and FMC estimation. The results indicated that, first, $SAI_{1200}$ was more suitable for estimating the EWT than FMC, whereas $SAI_{970}$ and $SAI_{1660}$ were more suitable for estimating the FMC. Second, $SAI_{1200}$ achieved the most accurate estimation of the EWT with a cross-validation coefficient of determination ($R_{cv}^2$) of 0.845 and relative cross-validation root mean square error ($rRMSE_{cv}$) of 8.90%. Third, $SAI_{1660}$ outperformed the other indices in estimating the FMC at the leaf level, with an $R_{cv}^2$ of 0.637 and $rRMSE_{cv}$ of 8.56%. Fourth, $SAI_{970}$ achieved a moderate accuracy in estimating the EWT ($R_{cv}^2$ of 0.25 and $rRMSE_{cv}$ of 19.68%) and FMC ($R_{cv}^2$ of 0.275 and $rRMSE_{cv}$ of 12.10%) at the leaf level. These results can enrich the application of the SAIs and demonstrate the potential of using $SAI_{1200}$ to determine the leaf EWT and $SAI_{1660}$ to obtain the leaf FMC among various plant types.

## Introduction

The vegetation water content (VWC) is a valuable indicator of vegetation drought stress [1], forest fire risk [2, 3], and regional water resource assessment [4]. The most accurate method to

evaluate the water status of vegetation involves traditional physiological measurements; however, this method is time consuming, laborious, and cannot meet the requirements of large-scale, real-time monitoring [5]. The development of remote sensing technology has enabled the prompt monitoring of the VWC in real time in a nondestructive manner over a large area [6]. The accurate evaluation of the VWC based on spectral reflectance measurements has always been a key research topic in remote sensing [7–15]. The main VWC parameters are the leaf level equivalent water thickness (EWT, g $cm^{-2}$), which is based on area, and the fuel moisture content (FMC), which is based on mass [16]. Most studies have aimed to develop techniques for or evaluate the use of the spectral reflectance to estimate the EWT [17–21]. Moreover, certain studies indicated that the spectral reflectance is highly correlated with the FMC [22–25].

At present, the main methods used to estimate the leaf water content based on statistical analysis include spectral indices [26–31], derivative spectra [24, 32] and post continuum removal indicators [33–35]. In this work, we focused on only the spectral indices. The vegetation spectral index is widely used to analyze the vegetation biophysical properties because of its simplicity and high generalizability. In the spectral domain (400–2500 nm), water absorption features, which appear at approximately 1200 nm, 970 nm, 1950 nm and 1450 nm [36, 37], are generally used to estimate the VWC [21, 38–40]. Moreover, certain studies reported a strong correlation between the reflectance spectra between 1650 and 1850 nm and water content of leaves [25, 36]. Based on these specific absorption values of water occurring across localized spectral regions of short wave infrared (SWIR) and near infrared (NIR) bands, many different vegetation water diagnostic indicators have been proposed, such as the water index (WI) [41], simple ratio water index (SRWI) [42], moisture stress index (MSI) [43], three-band ratio indices ($RATIO_{975}$ and $RATIO_{1200}$) [24], normalized difference water index (NDWI) [10], normalized difference infrared index (NDII) [44], global vegetation moisture index (GVMI) [45], relative depth index (RDI) [32], and depth water index (DWI) [46]. Although these indices have been successfully used to estimate the EWT and FMC at the leaf or canopy levels [35, 42–44, 47, 48], the indices were developed only considering two or three specific bands (e.g., the WI, SRWI, MSI, NDWI, NDII, GVMI) or to examine a specific plant species. For example, Pu et al. [29] used two three-band ratio indices ($RATIO_{975}$ and $RATIO_{1200}$) to assess the water status (leaf FMC) of oak leaves by considering the water absorption characteristics in the range of 920–1110 nm and 1090–1285 nm, respectively. Delegido Pasqualotto et al. [46] proposed the DWI to accurately predict the EWT at the canopy level within regions covered by different crop types. However, the DWI was calculated considering only four specific bands for all leaves.

The indices proposed in the abovementioned studies were calculated considering the same specific bands for all leaves, and the differences in the spectral absorption characteristics among different leaves, especially those of different vegetation species were mostly ignored. However, the contents of water and other components vary among different leaves, and this phenomenon may lead to the location deviation of the peaks or troughs of the spectral absorption features. Spectral absorption characteristics represent a valuable tool to study the composition and content of substances by remote sensing technology. Previous studies have shown that the spectral absorption index (SAI), which was first proposed by Wang et al. [49] and applied to remote sensing geology, can reflect the variation characteristics of the spectral absorption features [50]. To realize mineral mapping, Wang et al. [49] defined certain SAIs and used $SAI_{2175}$ and $SAI_{2295}$ to extract alteration tuff and altered basalt information, respectively, from far-ultraviolet imaging spectrograph images in the Hatu Mining Area. Recently, Li et al. [51] reported that $SAI_{680}$ was the most sensitive to changes in the fraction of absorption

photosynthetically active radiation (FAPAR) compared to those in the absorption peak depth (ad), absorption peak symmetry (AA) and NDVI. These previous studies indicated that more accurate retrieval results could be obtained using SAIs owing to the consideration of the continuous reflectance curve characteristics of different leaves rather instead of several specific bands for all leaves. However, to date, the application of SAI in estimating the VWC has not been reported. Therefore, this study aims to develop a new SAI that not only considers the spectral reflectance heterogeneity of different leaves but can also be used for various plant species. Moreover, the accuracies of the new SAIs and abovementioned ten typical spectral indices in estimating the leaf EWT and FMC are compared.

## Materials and methods

### Data collection

The study area was located in the Chengdu University of Technology, Sichuan Province, China. Three species of trees (camphor (VX), capricorn (VJ), red-leaf plum (VL)) were selected for leaf sampling in the sample area under clear and cloudless weather on May 15, 2019. Overall, 292 leaf samples in the tree crowns were collected. The capricorn (VJ) and red-leaf plum (VL) trees had only new leaves, while the camphor tree (VX) had both new and mature leaves. The collected samples were immediately sealed in plastic bags and transported to the laboratory in a cooler at 5˚C.

### Water content and leaf reflectance measurements

Under controlled laboratory conditions, leaf weight and spectral reflectance measurements were collected to reduce any possible error caused by changing atmospheric conditions. To avoid the influence of high temperatures on the water content of leaves during the contact spectrum measurement, the fresh weight (FW, g) of each leaf was first measured. Next, the spectral data of each leaf were obtained using a FieldSpec® 3 field spectroradiometer (ASD, Inc.; Boulder, Colorado) with a wide spectral range (350 to 2500 nm). During the spectral measurement process, blackout curtains were used to shade the window, and the leaves were placed on black flannelette to ensure that the only light source pertained to the measurement instrument. The spectral values of the upper, middle and lower parts of each leaf were measured, and the mean of the three measurements was considered as the spectral value of the leaf. Next, the leaves were scanned, and digital processing was conducted in MapGIS to obtain the area of each leaf polygon (A, $cm^2$). Finally, all the leaves were dried at 80˚C to obtain the dry weight (DW, g).

### Calculation of the vegetation water indices

The EWT [33] and FMC were calculated using Eqs (1) and (2), respectively.

$$EWT = \frac{FW - DW}{A}, \tag{1}$$

$$FMC = \frac{FW - DW}{FW} \times 100\%, \tag{2}$$

where FW and DW indicate the fresh and dry mass of each leaf (g), respectively, and $A$ is the leaf area ($cm^2$).

## Development of the new SAIs

The spectral absorption feature was composed of the spectral absorption peak (wavelength position of the minimum reflectance of an absorption feature, point m in Fig 1) and two spectral absorption shoulder ends ($S_1$ and $S_2$ in Fig 1). The line between $S_1$ and $S_2$ was defined as the nonabsorption baseline, as shown in Fig 1. Wang et al. [49] defined the SAI as the ratio of the reflectance of the nonabsorption baseline at the wavelength position of the spectral band to that at the spectral absorption peak ($SAI = {}^{\rho_M}/_{\rho_m}$; $\rho_M$ and $\rho_m$ are shown in Fig 1).

According to the water absorption features and the SAI technique proposed by Wang et al. [49], we defined three new SAIs: $SAI_{970}$, $SAI_{1200}$, and $SAI_{1660}$.

Fig 2 shows the three absorption bands at approximately 970 nm (915–1085 nm), 1200 nm (1085–1265 nm) and 1660 nm (1630–1690 nm) and the nonabsorption baseline formed by the shoulders of these bands, which were used to calculate the new SAIs in this study.

The three SAIs ($SAI_{970}$, $SAI_{1200}$, and $SAI_{1660}$) were calculated using Eqs (3) and (4) [49], in which $d$ is the absorption symmetry parameter (Eq (3)). The ten spectral indices based on the water absorption bands were calculated according to the formulas listed in Table 1.

$$d = (\lambda_2 - \lambda_m)/(\lambda_2 - \lambda_1), \tag{3}$$

$$SAI = \frac{d \times \rho_1 + (1 - d) \times \rho_2}{\rho_m}. \tag{4}$$

$\rho$ is the spectral reflectance; $\overline{\rho}_{\lambda_1-\lambda_2}$ is the average spectral reflectance in the $\lambda_1$-$\lambda_2$ region; $\min(\rho_{1120-1150})$ is the minimum spectral reflectance in the band range of 1120 nm to 1250 nm; and $y_i (i = 1,2)$ is calculated for $x_i (x_1 = 970, x_2 = 1200)$ as

$$y_i = \frac{(\rho_{1080} - \rho_{850})}{230} * x_i + \frac{(\rho_{1080} * 850 - \rho_{850} * 1080)}{-230} \tag{5}$$

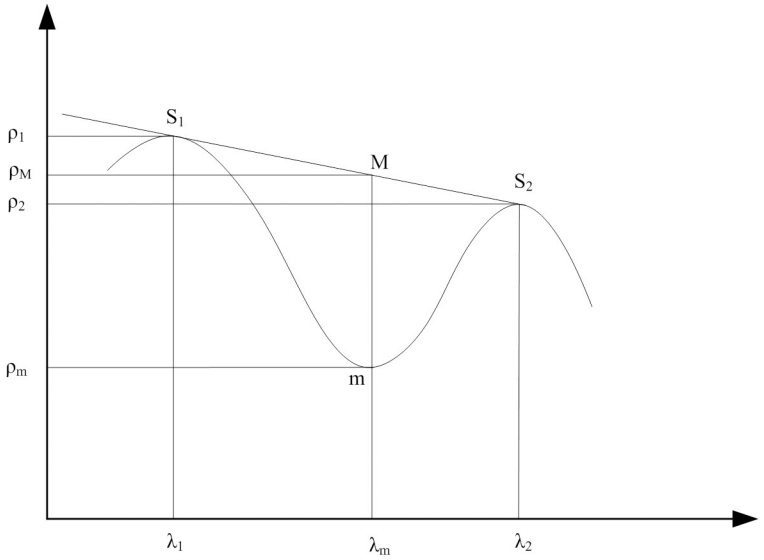


**Fig 1. Spectral absorption feature.** m is the Spectral Absorption Peak; $S_1$ and $S_2$ are Shoulders; $\lambda$ is the Corresponding Wavelength; $\rho$ is the Spectral Reflectance.

https://doi.org/10.1371/journal.pone.0249351.g001

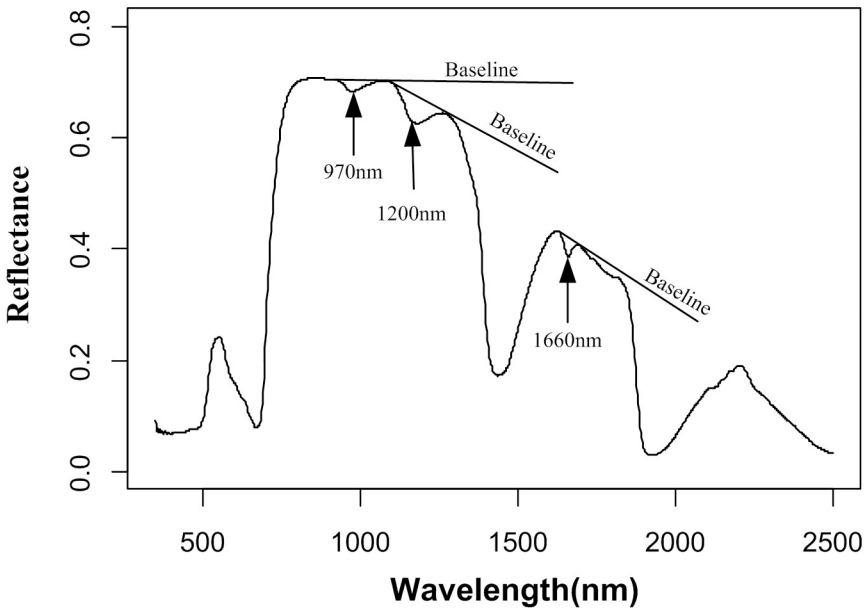


**Fig 2. Typical reflectance spectrum of the sample (three absorption bands and nonabsorption baselines).**

https://doi.org/10.1371/journal.pone.0249351.g002

Due to the differences in the vegetation species and internal structures, the absorption peaks or shoulders of all the leaves varied. Therefore, the key problem associated with the SAI calculations was to identify the absorption peak band ($\lambda_m$ in Fig 1) and shoulders ($\lambda_1$ and $\lambda_2$ in Fig 1). In this study, the positions of the absorption peak and shoulders were obtained by calculating the minimum and maximum spectral reflectance values of each leaf in different bands by using R 4.0.1.

The performance of each index was tested using various fitting functions: linear, polynomial, and exponential functions.

## Validation strategy

To obtain robust results, the k-fold cross-validation method was used in this study. The basic principle of this technique can be described as follows [52]. First, the original dataset is divided into k subsets of approximately the same size. Second, the first dataset is used as the validation dataset, and the remaining k-1 datasets are combined to estimate the model parameters. Based on the model parameters, the dependent variables of the validation dataset are predicted, and the squared sum of the prediction errors is calculated. Third, the cross-validation process is repeated k times with each of the k subdatasets used as a validation dataset. In this study, we adopted a 10-fold (k = 10) cross-validation procedure.

The reliability of the indices for estimating the leaf EWT and FMC was evaluated considering the cross-validated coefficient of determination ($R_{cv}^2$) and relative cross-validated root mean square error ($rRMSE_{cv}$). All the analyses were implemented in R 4.0.1. The $rRMSE_{cv}$ was calculated using Eq (6).

$$rRMSE_{cv} = \frac{RMSE_{cv}}{\overline{EWT} or \overline{FMC}} \tag{6}$$

where $\overline{EWT}$ and $\overline{FMC}$ are the average values of the measured leaf EWT and FMC, respectively.

**Table 1. Spectral reflectance indices to estimate the water content and related source references.**

| Spectral index | Spectral index | Calculation formula | Reference |
|---|---|---|---|
| WI | Water Index | $\frac{\rho_{900}}{\rho_{970}}$ | PeÑUelas et al. [23] |
| SRWI | Simple Ratio Water Index | $\frac{\rho_{858}}{\rho_{1240}}$ | Zarco-Tejada et al. [42] |
| $NDWI_{1240}$ | Normalized Difference Water Index (NDWI) | $\frac{(\rho_{860}-\rho_{1240})}{(\rho_{860}+\rho_{1240})}$ | Stimson et al. [35] |
| RDI | Relative Depth Index | $\frac{(\rho_{1116}-\min(\rho_{1120-1150}))}{\rho_{1116}}$ | Rollin and Milton [32] |
| $RATIO_{975}$ | Three-Band Ratio Index | $\frac{2\overline{\rho}_{960-990}}{(\overline{\rho}_{920-940}+\overline{\rho}_{1090-1100})}$ | Pu et al. [24] |
| $RATIO_{1200}$ | Three-Band Ratio Index | $\frac{2\overline{\rho}_{1180-1220}}{(\overline{\rho}_{1090-1110}+\overline{\rho}_{1265-1285})}$ | Pu et al. [24] |
| DWI | Depth Water Index | $(y_1-\rho_{970})+(y_2-\rho_{1200})$ | Pasqualotto et al. [46] |
| MSI | Moisture Stress Index | $\frac{\rho_{1600}}{\rho_{820}}$ | Hunt and Rock [43] |
| NDII | Normalized Difference Infrared Index | $\frac{(\rho_{860}-\rho_{1600})}{(\rho_{860}+\rho_{1600})}$ | Hardisky et al. [44] |
| GVMI | Global Vegetation Moisture Index | $\frac{(\rho_{820}+0.1)-(\rho_{1600}+0.02)}{(\rho_{820}+0.1)+(\rho_{1600}+0.02)}$ | Ceccato et al. [45] |

https://doi.org/10.1371/journal.pone.0249351.t001

# Results

## Statistics of the measured plant variables

In this study, 292 samples acquired from three plant species were used. Within the sample sites, the water content of leaves exhibited considerably variability: the EWT and FMC ranged from 0.006 g $cm^{-2}$ to 0.016 g $cm^{-2}$ and from 45.16% to 82.72% (Table 2), respectively. In addition, the leaf EWT and FMC among the three tree species were significantly different (Fig 3), with the highest EWT and FMC value of 0.016 and 82.72%, respectively, corresponding to VX and the lowest EWT and FMC values corresponding to VJ (0.006) and VX (45.16%).

## Retrieval of the EWT from the new SAIs

The leaf EWT was estimated using linear, polynomial and exponential functions. The results (Table 3) showed that (1) except for the RDI and $RATIO_{975}$, all the indices exhibited a significant correlation with the EWT at the 0.01 level, even though the DWI and $SAI_{1660}$ exhibited a less significant correlation with the EWT. (2) $SAI_{1200}$, $RATIO_{1200}$, the GVMI, the MSI and the NDII outperformed the other indices in estimating the EWT, with $R_{cv}^2$ values greater than 0.740 and $rRMSE_{cv}$ values less than 11.41%. The optimal result was obtained using $SAI_{1200}$, as indicated by the highest $R_{cv}^2$ of 0.845 and lowest $rRMSE_{cv}$ of 8.90% in the linear fitting results (Fig 4), followed by that obtained using $RATIO_{1200}$ with an $R_{cv}^2$ of 0.831 and an $rRMSE_{cv}$ of 9.28% (Fig 4).

**Table 2. Statistics of the leaf EWT and FMC for the samples.**

| Species | Variable | Min | Max | Mean | Std. Deviation | N |
|---|---|---|---|---|---|---|
| Pooled data | EWT (g $cm^{-2}$) | 0.006 | 0.016 | 0.010 | 0.002 | 292 |
| | FMC (%) | 45.16 | 82.72 | 64.03 | 0.091 | |
| VJ | EWT | 0.006 | 0.010 | 0.008 | 0.001 | 46 |
| | FMC | 57.40 | 67.20 | 61.60 | 0.025 | |
| VL | EWT | 0.006 | 0.013 | 0.008 | 0.002 | 66 |
| | FMC | 62.60 | 77.50 | **69.60** | 0.036 | |
| VX | EWT | 0.008 | 0.016 | **0.012** | 0.001 | 180 |
| | FMC | 45.16 | 82.72 | 62.60 | 0.107 | |

https://doi.org/10.1371/journal.pone.0249351.t002

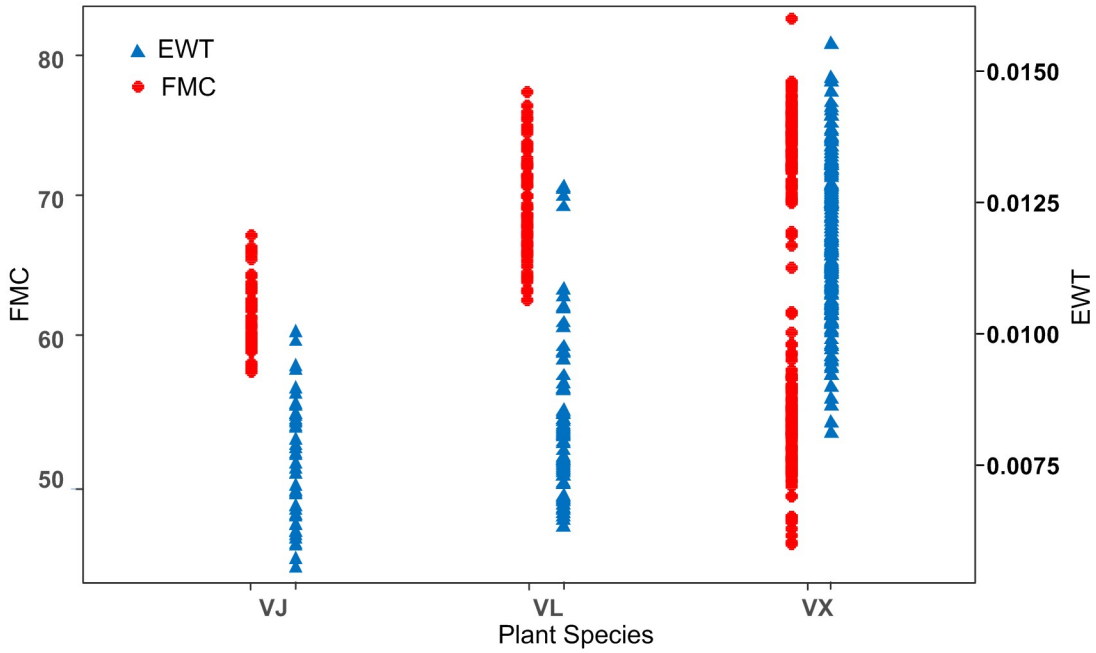


**Fig 3. Leaf EWT (g cm$^{-2}$) and FMC (%) of the three plant species.**

https://doi.org/10.1371/journal.pone.0249351.g003

## Retrieval of the FMC from the new SAIs

The FMC was significantly correlated with all the indices except the GVMI and $RATIO_{1200}$ at the 0.01 level for the pooled data (Table 4). $SAI_{1660}$, $SAI_{970}$, $RATIO_{975}$, the RDI, and the DWI were more sensitive to the FMC than the EWT. $SAI_{1660}$ achieved the optimal estimation of the FMC, as indicated by the highest $R_{cv}^2$ of 0.637 and lowest $rRMSE_{cv}$ of 8.56% in the polynomial fitting results, followed by the RDI ($R_{cv}^2$ of 0.461 and $rRMSE_{cv}$ of 10.43%) (Fig 5).

**Table 3. Performance of the regression models in estimating the leaf equivalent thickness (EWT, g cm$^{-2}$).**

| Index | EWT | | | |
|---|---|---|---|---|
| | P | Regression Equation | $Rcv^2$ | *rRMSEcv* |
| $SAI_{1200}$ | <0.0001 | y = 0.204*x-0.205 | 0.845 | 8.90% |
| $RATIO_{1200}$ | <0.0001 | y = -0.197*x+0.198 | 0.831 | 9.28% |
| GVMI | <0.0001 | y = 0.042*x+0.001 | 0.76 | 11.04% |
| MSI | <0.0001 | y = 0.033*$x^2$-0.073*x+0.046 | 0.746 | 11.39% |
| NDII | <0.0001 | y = 0.038*x+0.0038 | 0.744 | 11.41% |
| WI | <0.0001 | y = 0.186*x-0.179 | 0.518 | 15.68% |
| NDWI | <0.0001 | y = 0.762*$x^2$+0.058*x+0.009 | 0.355 | 18.13% |
| SRWI | <0.0001 | y = 0.165*$x^2$-0.302*x+0.146 | 0.35 | 18.20% |
| $SAI_{970}$ | <0.0001 | y = 0.100*x-0.093 | 0.25 | 19.68% |
| DWI | <0.0001 | y = 0.032*x+0.007 | 0.113 | 21.27% |
| $SAI_{1660}$ | <0.001 | y = -0.015*x+0.027 | 0.04 | 22.14% |
| RDI | n.s. | - | - | - |
| $RATIO_{975}$ | n.s. | - | - | - |

$rRMSE_{cv}$ is the Relative Cross-Validated Root Mean Square Error, and $R_{cv}^2$ is the Cross-Validated Coefficient of Determination.
n.s.: not significant at the 0.05 level ($n$ = 292).

https://doi.org/10.1371/journal.pone.0249351.t003

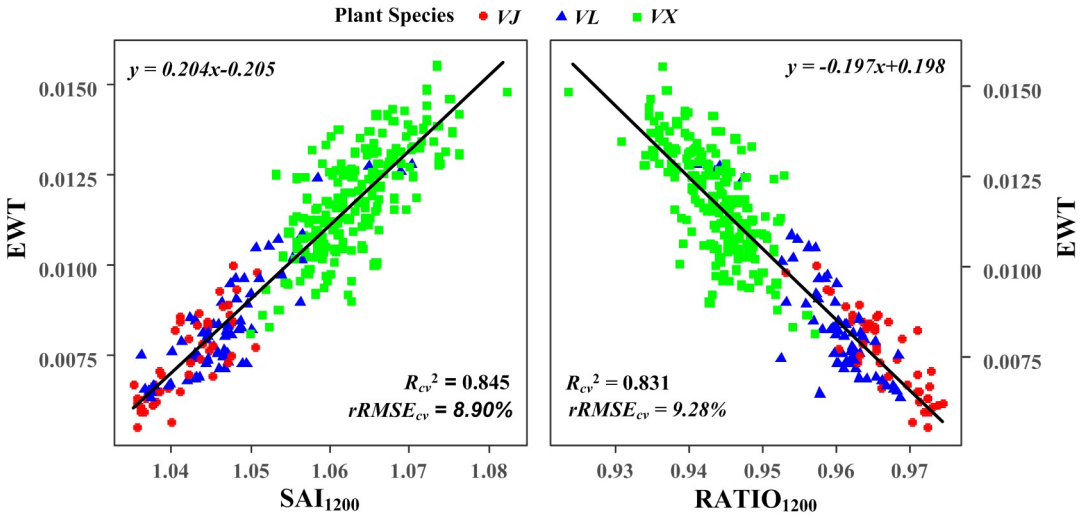


**Fig 4. Relationships between the measured EWT and $SAI_{1200}$ (left)/$RATIO_{1200}$ (right) for the pooled data.**

https://doi.org/10.1371/journal.pone.0249351.g004

## Discussion

### Performance of the new SAIs in retrieving the water content

In this study, three new spectral absorption indices ($SAI_{970}$, $SAI_{1200}$, and $SAI_{1660}$) were used to retrieve the leaf EWT and FMC from the reflectance spectra over three plant types dataset. To our knowledge, this study represents the first attempt to develop such SAIs for retrieving the leaf water content. The SAI is the ratio of the reflection intensity of the nonabsorption baseline at the wavelength position of the spectral band to that at the bottom of the spectral band. This ratio can also be defined as the "relative absorption depth".

**Table 4. Performance of the regression models for estimating the leaf FMC (%).**

| Index | FMC | | | |
|---|---|---|---|---|
| | P | Regression Equation | $Rcv^2$ | *rRMSEcv* |
| SAI1660 | <0.0001 | y = -26.346*x$^2$+58.963*x-32.200 | 0.637 | 8.56% |
| RDI | <0.0001 | y = -1.864*x$^2$-0.218*x+0.500 | 0.461 | 10.43% |
| WI | <0.0001 | y = 122.29*x$^2$-242.87*x+125.15 | 0.32 | 11.73% |
| SAI970 | <0.0001 | y = 4.119*x-3.616 | 0.275 | 12.10% |
| DWI | <0.0001 | y = -14.154*x$^2$+4.520*x+0.345 | 0.235 | 12.43% |
| SAI1200 | <0.0001 | y = 297.64*x$^2$-627*x+330.93 | 0.138 | 13.20% |
| RATIO975 | <0.0001 | y = -105.37*x$^2$+200.88*x-95.061 | 0.135 | 13.22% |
| SRWI | <0.0001 | y = 0.643*x-0.016 | 0.074 | 13.67% |
| NDWI | <0.0001 | y = 1.289*x+0.627 | 0.071 | 13.69% |
| NDII | <0.0001 | y = 6.791*x$^2$-1.972*x+0.760 | 0.049 | 13.86% |
| MSI | <0.001 | y = 2.804*x$^2$-4.240*x+2.219 | 0.04 | 13.94% |
| RATIO1200 | n.s. | - | - | - |
| GVMI | n.s. | - | - | - |

$rRMSE_{cv}$ is the Relative Cross-Validated Root Mean Square Error, and $R_{cv}^2$ is the Cross-Validated Coefficient of Determination.
n.s.: not significant at the 0.05 level ($n$ = 292).

https://doi.org/10.1371/journal.pone.0249351.t004

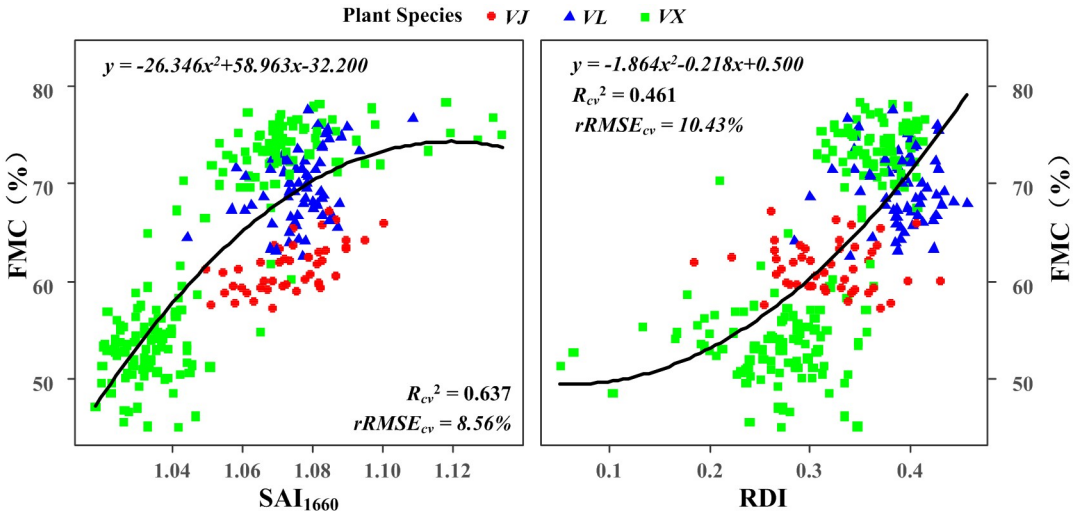


**Fig 5. Relationships between the measured leaf FMC and $SAI_{1660}$ (left)/RDI (right) for the pooled data.**

https://doi.org/10.1371/journal.pone.0249351.g005

As shown in Table 3, the EWT was positively correlated with $SAI_{1200}$ and $SAI_{970}$, but negatively correlated with $SAI_{1660}$ for the pooled data. This phenomenon occurred because $SAI_{1200}$ and $SAI_{970}$ represent the relative absorption depth of the vegetation water near 970 nm and 1200 nm, respectively, and both indices are expected to increase with an increase in the leaf water content. In contrast, the absorption characteristic near 1660 nm is related to the leaf dry matter constituents (e.g. lignin and cellulose) that become prominent as the water content decreases [29, 53]. This aspect also explains why $SAI_{1660}$ was more closely related to the mass based parameter FMC than the area based parameter EWT. According to this principle, FMC was more likely to be species dependent than EWT, as discussed in the following section.

Among the indices, the new spectral absorption index $SAI_{1200}$ was the most suitable index for estimating the EWT at the leaf level, as indicated by the $R_{cv}^2$ of 0.845 and $rRMSE_{cv}$ of 8.90%. However, $SAI_{970}$ achieved only a moderate accuracy in predicting the EWT at the leaf level. The results were consistent with those reported by Kovar et al. [5] who indicated that compared to that at 1200 nm, the absorption characteristic at 970 nm showed relatively weaker sensitivity to the leaf EWT in their study on soybean plants. This phenomenon likely occurred because the absorption characteristic of water at 970 nm is weaker than that at 1200 nm; moreover, the reflectance at 970 nm is more significantly affected by the vegetation structure and other factors (leaf structure and dry matter content) than that at 1200 nm [47]. This aspect is likely why $SAI_{970}$ exhibits a slightly stronger correlation with FMC than $SAI_{1200}$, because FMC is a mass based parameter and has a stronger correlation with dry matter than EWT.

In terms of the traditionally simple or normalized ratio index configured with only a few specific spectral bands, significant relationships were observed between the EWT and GVMI, MSI, NDII ($R_{cv}^2 > 0.70$), while weaker correlations were achieved with WI, NDWI, SRWI ($R_{cv}^2 < 0.55$). The results are consistent with those of other studies, which indicated that the spectral indices involving the combination of the SWIR and NIR wavelengths were more effective to estimate the leaf EWT than those that only combined the NIR wavelengths [33, 47, 54]. However, compared with $SAI_{1200}$ and $RATIO_{1200}$, these indices were suboptimal, and $SAI_{1200}$ and $RATIO_{1200}$ combined only the NIR wavelengths. The results demonstrate that selecting an appropriate vegetation index in the NIR bands can effectively indicate the change in the leaf water content, especially among the indices derived from the absorption feature bands near

1200 nm. This phenomenon occurs because more notable water absorption characteristic exist near 1200 nm than at 970 nm [6].

The data in Table 4 show that $SAI_{1660}$ is the most strongly correlated with the leaf FMC, as indicated by the $R_{cv}^2$ of 0.637 and $rRMSE_{cv}$ of 8.56%. The other indices except for the GVMI and $RATIO_{1200}$ are only slightly related to the leaf FMC ($R_{cv}^2 < 0.50$). Our results confirm that the traditionally spectral indices are more suitable for estimating the EWT than the FMC at the leaf level [33, 54].

Furthermore, the results demonstrate that $SAI_{1200}$ and $SAI_{1660}$ can represent the variation characteristics of the spectral absorption features and help estimate the leaf water content. The high performance of the $SAI_{1200}$ and $SAI_{1660}$ can be attributed to the fact that the SAIs were constructed considering the symmetry in the absorption characteristics and spectral reflectance heterogeneity of different leaves; moreover, the SAI could eliminate the spectral contribution of the nonabsorbent materials through the nonabsorption baseline equation and ratio processing and measure the relative spectral absorption depth of water or dry matter components.

## Comparison of the SAIs and RATIO indices

**Similarity in the SAIs and RATIO indices.** The methods to establish the SAIs ($SAI_{970}$ and $SAI_{1200}$) and RATIO indices ($RATIO_{975}$ and $RATIO_{1200}$) were similar, and the values were obtained by calculating the ratio of the absorption bands near 970 nm and 1200 nm and the corresponding absorption shoulder bands. Both $SAI_{970}$ and $RATIO_{975}$ were more sensitive to the FMC than the EWT, whereas $SAI_{1200}$ and $RATIO_{1200}$ were more sensitive to the EWT.

To demonstrate the similarity, the FMC estimated using $SAI_{970}$ and EWT estimated using $SAI_{1200}$ were plotted against the FMC values estimated using $RATIO_{975}$ and EWT values estimated using $RATIO_{1200}$ (Fig 6). The similarity between $SAI_{1200}$ and $RATIO_{1200}$ was more notable than that between $SAI_{970}$ and $RATIO_{975}$, as indicated by the $R_{cv}^2$ values of 0.943 and 0.333, respectively. This difference might be interpreted as follows. The reflectivity of the absorption band at 970 nm was more significantly affected by other factors (leaf structure and dry matter content) than that of the absorption band at 1200 nm, thereby increasing the difference in the reflectivity of the absorption band at 970 nm among different leaves [47].

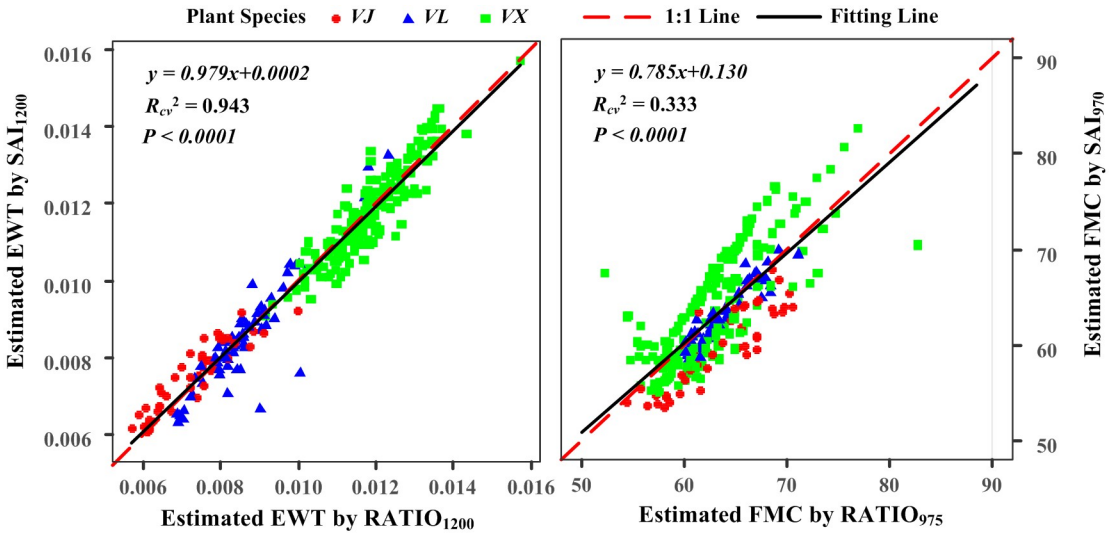


**Fig 6. Plots of the EWT and FMC estimated using RATIO and SAI for the pooled data.**

https://doi.org/10.1371/journal.pone.0249351.g006

Therefore, the similarity between $RATIO_{975}$ calculated with the same three specific bands for all leaves and $SAI_{970}$ calculated with the absorption peak and shoulders of individual leaves was not significant. In other words, the absorption characteristics at 970 nm were more susceptible to other factors, including water, than those at the absorption band at 1200 nm.

## Superiority of the SAIs over the RATIO indices

In this study, the SAIs ($SAI_{970}$ and $SAI_{1200}$) could more accurately estimate the FMC and EWT than the RATIO indices ($RATIO_{975}$ and $RATIO_{1200}$) (Table 2) since the SAIs were constructed considering the symmetry in the absorption characteristics and spectral reflectance heterogeneity of different leaves, which were not considered when constructing the RATIO indices. Moreover, the SAIs were calculated considering the absorption peak and absorption shoulder band of each leaf, whereas the RATIO indices were calculated considering the average spectral reflectance in a specific band range. Pu et al. [29] reported that the absorption position shifted to shorter wavelengths at 975 nm and 1200 nm and to a longer wavelength at 1750 nm as the leaf water content increased. However, using the average value in a specific band range as the value of the absorption feature peaks or troughs may obscure or weaken the change in the leaf spectral absorption feature induced by the water content.

## Inversion of the SAIs and RATIO indices for the leaf FMC

Pu et al. [29] found that $RATIO_{975}$ and $RATIO_{1200}$ outperformed the indices derived from the band at 1750 nm in evaluating the FMC. In our study, we obtained the opposite results. $SAI_{1660}$ outperformed the other indices in evaluating the FMC, as indicated by the $R_{cv}^2$ of 0.637 and an $rRMSE_{cv}$ of 8.56% in this study. However, $RATIO_{975}$ was weakly correlated with the FMC ($R_{cv}^2$ of 0.135 and $rRMSE_{cv}$ of 13.22%), and even at the 0.05 level, the correlation between $RATIO_{1200}$ and the FMC was not significant. The different results may be caused by the species differences because the water absorption band centered at 1750 nm (1650–1850 nm) is an indirect absorption band and is ascribed to chemicals such as cellulose, sugar and starch [29]. In addition, Pu et al. [29] analyzed the leaves of specific plant species (coastal live oak), whereas we used a multiplant dataset pooled with three plant species, specifically, camphor (VX), capricorn (VJ), and red-leaf plum (VL) trees.

## Dependency of the new SAIs on the plant species

Considering the influence of the plant species on the estimation of the water content parameters, we estimated the EWT of the three plant species considering $SAI_{1200}$ and $RATIO_{1200}$ (Fig 7). The estimation performances of $SAI_{1200}$ and $RATIO_{1200}$ for the three plant species were similar (Fig 7). The slopes of the linear regression lines for three plant species obtained with $SAI_{1200}$ ranged from 0.185 (VX) to 0.209 (VJ), and the intercept ranged from -0.211 (VJ) to -0.185 (VX). The ranges of the slope and intercept were 0.024 and 0.026, respectively.

The FMC of the three plant species was estimated using $SAI_{1660}$ and the RDI (Fig 8), and it was noted that the estimation performances of $SAI_{1660}$ and the RDI for the three plant species were considerably different (e.g., the quadratic coefficient of the quadratic equation for the three plant species obtained using $SAI_{1660}$ ranged from -37.98 (VX) to 23.04 (VL), and the coefficient of the primary term ranged from 84.35 (VX) to -48.13 (VL)). Expectedly, VX obtained the highest accuracy of leaf FMC estimation when using $SAI_{1660}$, followed by VJ. This phenomenon occurred because the spectral absorption characteristics of vegetation near the wavelength of 1660 nm become more notable with the decrease in the leaf FMC [29, 53]. Among the three species, the average FMC of VL was the highest (69.60%), and the corresponding values for VX (62.6%) and VJ (61.6%) were lower. Although the average FMC of VX

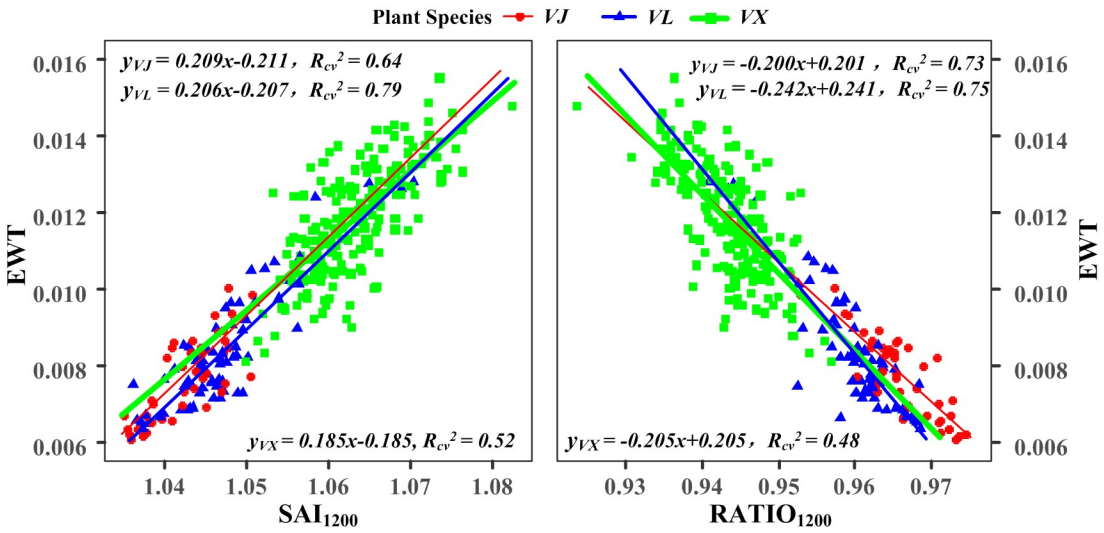


**Fig 7. Relationship between the measured EWT and $SAI_{1200}$ (left) and $RATIO_{1200}$ (right) at the species level.**

https://doi.org/10.1371/journal.pone.0249351.g007

was similar to that of VJ (or even slightly higher), VX could more accurately estimate the leaf FMC using $SAI_{1660}$, likely because of the wider changes in the FMC of VX (45.16% to 82.72%) than that of VJ (57.40% to 67.20%) and the larger sample size of the former parameter.

The correlation between the EWT and spectral indices from the pooled data was more significant than that between the EWT and those obtained from the data of individual species, as indicated by the $R_{cv}^2$ of 0.845 and 0.831 for $SAI_{1200}$ and $RATIO_{1200}$, respectively (Figs 4 and 7). However, the correlation between the FMC and spectral indices from the pooled data was not more significant than that between the FMC and those obtained from the data of the individual species (Figs 5 and 8). These phenomena indicated that the observed relationships between the FMC and reported spectral indices were more likely to be species specific than those between the EWT and spectral indices ($SAI_{1200}$ and $RATIO_{1200}$). In other words, the leaf

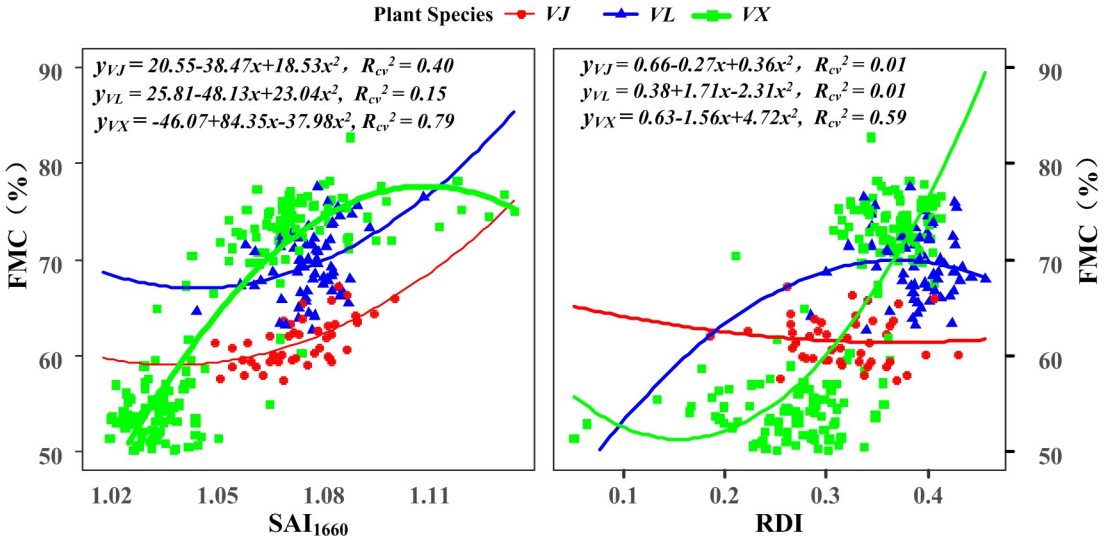


**Fig 8. Relationship between the measured FMC and $SAI_{1660}$ (left) and RDI (right) at the species level.**

https://doi.org/10.1371/journal.pone.0249351.g008

EWTs estimated using the spectral indices ($SAI_{1200}$ and $RATIO_{1200}$) were less influenced by variations in the internal leaf structures than the leaf FMCs estimated using the spectral indices ($SAI_{1660}$ and RDI).

### Importance of the FMC in estimating the leaf growth

The FMC is a mass based parameter. Pu et al. [24] noted that the data points of fresh green leaves and brown-gray leaves form two clusters in the scatter plots of several spectral features with the FMC. A similar phenomenon was observed in this study. A notable gap existed between the new leaves (green square dots in the top region in Fig 8) and mature leaves (green square dots in the bottom region in Fig 8) of the same plant species (VX), although this gap was not reflected in the EWT (Fig 7). This finding further confirmed that the mass based FMC parameter is important for estimating the leaf growth [16]. We speculate that the FMC might be more suitable for distinguishing the leaf water status at different growth stages than the EWT. To verify this aspect, additional work is necessary such as that involving the collection of leaf samples from different seasons and more plant species.

### Uncertainties

The SAI was compared with commonly used water vegetation indices; however, the corresponding approach was not compared with other methods (e.g., the use of derivative spectra and indicators after continuum removal and similarity matrix and artificial neural network methods). In addition, this study considered only three common vegetation types in the same season, and thus, the applicability of these indices to other vegetation types in different growing seasons must be examined in the future. Nevertheless, our research results provide a basis for subsequent research and confirm the application potential of SAIs in vegetation water retrieval. Moreover, this study demonstrates a novel concept for the hyperspectral inversion of vegetation water.

## Conclusions

Considering the symmetry of spectral absorption at 970 nm, 1200 nm and 1660 nm and spectral heterogeneity of different leaves, we proposed three new SAIs ($SAI_{970}$, $SAI_{1200}$, and $SAI_{1660}$) to retrieve the leaf EWT and FMC for various plant types. The following key conclusions were derived: (1) $SAI_{1200}$ was more suitable for estimating the EWT, whereas $SAI_{970}$ and $SAI_{1660}$ were more suitable for estimating the FMC. (2) $SAI_{970}$ and $SAI_{1200}$ outperformed $RATIO_{975}$ and $RATIO_{1200}$, respectively, in estimating the FMC and EWT. (3) The new SAIs ($SAI_{1200}$ and $SAI_{1660}$) can effectively estimate the leaf water content.

## Supporting information

**S1 File.**
(PDF)

**S2 File.**
(PDF)

**S1 Data.**
(CSV)

## Acknowledgments

The authors sincerely thank Dr. Xiaolu Tang (Chengdu University of Technology), the two reviewers and the editors of the PLOS ONE for their valuable comments and constructive

suggestions, which greatly helped to improve the quality of this manuscript. We also thank AJE for its linguistic assistance during the preparation of this manuscript.

## Author Contributions

**Conceptualization:** Hong Li.

**Data curation:** Hong Li, Junjie Lei, Jinxing She.

**Formal analysis:** Hong Li.

**Funding acquisition:** Wunian Yang.

**Investigation:** Hong Li, Junjie Lei.

**Methodology:** Hong Li, Wunian Yang.

**Project administration:** Wunian Yang.

**Resources:** Junjie Lei, Jinxing She.

**Software:** Jinxing She.

**Supervision:** Xiangshan Zhou.

**Validation:** Hong Li.

**Visualization:** Xiangshan Zhou.

**Writing – original draft:** Hong Li.

## References

1. El-Hendawy SE, Al-Suhaibani NA, Elsayed S, Hassan WM, Dewir YH, Refay Y, et al. Potential of the existing and novel spectral reflectance indices for estimating the leaf water status and grain yield of spring wheat exposed to different irrigation rates. Agric Water Manag. 2019; 217: 356–373.
2. Myoung B, Kim S, Nghiem S, Jia S, Whitney K, Kafatos M. Estimating live fuel moisture from MODIS satellite data for wildfire danger assessment in Southern California USA. Remote Sens. 2018; 10: 87.
3. Arganaraz JP, Landi MA, Bravo SJ, Gavier-Pizarro GI, Scavuzzo CM, Bellis LM. Estimation of live fuel moisture content from MODIS images for fire danger assessment in Southern Gran Chaco. IEEE J Sel Top Appl Earth Obs Remote Sens. 2016; 9: 5339–5349.
4. García-Haro FJ, Campos-Taberner M, Moreno Á, Tagesson HT, Camacho F, Martínez B, et al. A global canopy water content product from AVHRR/Metop. ISPRS J Photogramm Remote Sens. 2020; 162: 77–93.
5. Kovar M, Brestic M, Sytar O, Barek V, Hauptvogel P, Zivcak M. Evaluation of hyperspectral reflectance parameters to assess the leaf water content in soybean. Water. 2019; 11: 443.
6. Fang M, Ju W, Zhan W, Cheng T, Qiu F, Wang J. A new spectral similarity water index for the estimation of leaf water content from hyperspectral data of leaves. Remote Sens Environ. 2017; 196: 13–27.
7. Ali A, Khurshid K, Ullah S, Arshad M. Estimation of leaf water content from mid- and thermal-infrared spectra by coupling genetic algorithm and partial least squares regression. J Appl Remote Sens. 2018; 12: 1.
8. Chen S, Chen Y, Chen J, Zhang Z, Fu Q, Bian J, et al. Retrieval of cotton plant water content by UAV-based vegetation supply water index (VSWI). Int J Remote Sens. 2020; 41: 4389–4407.
9. El-Hendawy SE, Al-Suhaibani NA, Hassan WM, Dewir YH, Elsayed S, Al-Ashkar I, et al. Evaluation of wavelengths and spectral reflectance indices for high-throughput assessment of growth, water relations and ion contents of wheat irrigated with saline water. Agric Water Manag. 2019; 212: 358–377.
10. Gao BC. NDWI—a normalized difference water index for remote sensing of vegetation liquid water from space. Remote Sens Environ. 1996; 58: 257–266.
11. Hunt E, Li L, Friedman J, Gaiser P, Twarog E, Cosh M. Incorporation of stem water content into vegetation optical depth for crops and woodlands. Remote Sens. 2018; 10: 273.

12. Zhang C, Pattey E, Liu J, Cai H, Shang J, Dong T. Retrieving leaf and canopy water content of winter wheat using vegetation water indices. IEEE J Sel Top Appl Earth Obs Remote Sens. 2018; 11: 112–126.

13. Zhang F, Zhou G. Estimation of vegetation water content using hyperspectral vegetation indices: a comparison of crop water indicators in response to water stress treatments for summer maize. BMC Ecol. 2019; 19: 18. https://doi.org/10.1186/s12898-019-0233-0 PMID: 31035986

14. Zhang L, Zhou Z, Zhang G, Meng Y, Chen B, Wang Y. Monitoring the leaf water content and specific leaf weight of cotton (Gossypium hirsutum L.) in saline soil using leaf spectral reflectance. Eur J Agron. 2012; 41: 103–117.

15. Zhang L, Zhou Z, Zhang G, Meng Y, Chen B, Wang Y. Monitoring cotton (Gossypium hirsutum L.) leaf ion content and leaf water content in saline soil with hyperspectral reflectance. Eur J Remote Sens. 2014; 47: 593–610.

16. Neinavaz E, Skidmore AK, Darvishzadeh R, Groen TA. Retrieving vegetation canopy water content from hyperspectral thermal measurements. Agric For Meteorol. 2017; 247: 365–375.

17. Deffet S, Farace P, Macq B. Sparse deconvolution of proton radiography data to estimate water equivalent thickness maps. Med Phys. 2020; 47: 509–517. https://doi.org/10.1002/mp.13917 PMID: 31705805

18. Lei J, Yang W, Li H, Wu M, She J, Zhou X, et al. Leaf equivalent water thickness assessment by means of spectral analysis and a new vegetation index. J Appl Remote Sens. 2019; 13: 1.

19. Ma J, Huang S, Li J, Li X, Song X, Leng P, et al. Estimating vegetation water content of corn and soybean using different polarization ratios based on L- and S-band radar data. IEEE Geosci Remote Sens Lett. 2017; 14: 364–368.

20. Rodríguez-Pérez JR, Ordóñez C, González-Fernández AB, Sanz-Ablanedo E, Valenciano JB, Marcelo V. Leaf water content estimation by functional linear regression of field spectroscopy data. Biosyst Eng. 2018; 165: 36–46.

21. Wocher M, Berger K, Danner M, Mauser W, Hank T. Physically-based retrieval of canopy equivalent water thickness using hyperspectral data. Remote Sens. 2018; 10: 1924.

22. Jin X, Shi C, Yu CY, Yamada T, Sacks EJ. Determination of leaf water content by visible and near-infrared spectrometry and multivariate calibration in miscanthus. Front Plant Sci. 2017; 8: 721. https://doi.org/10.3389/fpls.2017.00721 PMID: 28579992

23. PeÑUelas J, Filella I, Biel C, Serrano L, Savé R. The reflectance at the 950–970 nm region as an indicator of plant water status. Int J Remote Sens. 2007; 14: 1887–1905.

24. Pu R, Foschi L, Gong P. Spectral feature analysis for assessment of water status and health level in coast live oak (Quercus agrifolia) leaves. Int J Remote Sens. 2010; 25: 4267–4286.

25. Tian Q, Tong Q, Pu R, Guo X, Zhao C. Spectroscopic determination of wheat water status using 1650–1850 nm spectral absorption features. Int J Remote Sens. 2010; 22: 2329–2338.

26. Chakroun H, Mouillot F, Hamdi A. Regional equivalent water thickness modeling from remote sensing across a tree cover/LAI gradient in mediterranean forests of Northern Tunisia. Remote Sens. 2015; 7: 1937–1961.

27. Hunt ER, Daughtry CST, Li L. Feasibility of estimating leaf water content using spectral indices from WorldView-3's near-infrared and shortwave infrared bands. Int J Remote Sens. 2015; 37: 388–402.

28. Liu L, Zhang S, Zhang B. Evaluation of hyperspectral indices for retrieval of canopy equivalent water thickness and gravimetric water content. Int J Remote Sens. 2016; 37: 3384–3399.

29. Pu R, Ge S, Kelly NM, Gong P. Spectral absorption features as indicators of water status in coast live oak (Quercus agrifolia) leaves. Int J Remote Sens. 2010; 24: 1799–1810.

30. Wang L, Hunt ER, Qu JJ, Hao X, Daughtry CST. Remote sensing of fuel moisture content from ratios of narrow-band vegetation water and dry-matter indices. Remote Sens Environ. 2013; 129: 103–110.

31. Zhang JH, Xu Y, Yao FM, Wang PJ, Guo WJ, Li L, et al. Advances in estimation methods of vegetation water content based on optical remote sensing techniques. Sci China Technol Sci. 2010; 53: 1159–1167.

32. Rollin EM, Milton EJ. Processing of high spectral resolution reflectance data for the retrieval of canopy water content information. Remote Sens Environ. 1998; 65: 86–92.

33. Colombo R, Meroni M, Marchesi A, Busetto L, Rossini M, Giardino C, et al. Estimation of leaf and canopy water content in poplar plantations by means of hyperspectral indices and inverse modeling. Remote Sens Environ. 2008; 112: 1820–1834.

34. Kokaly RF, Despain DG, Clark RN, Livo KE. Mapping vegetation in Yellowstone national park using spectral feature analysis of AVIRIS data. Remote Sens Environ. 2003; 84: 437–456.

35. Stimson HC, Breshears DD, Ustin SL, Kefauver SC. Spectral sensing of foliar water conditions in two co-occurring conifer species: *Pinus edulis* and *Juniperus monosperma*. Remote Sens Environ. 2005; 96: 108–118.

36. Danson FM, Steven MD, Malthus TJ, Clark JA. High-spectral resolution data for determining leaf water content. Int J Remote Sens. 1992; 13: 461–470.

37. Tucker CJ. Remote sensing of leaf water content in the near infrared. Remote Sens Environ. 1979; 10: 23–32.

38. Cernicharo J, Verger A, Camacho F. Empirical and physical estimation of canopy water content from CHRIS/PROBA data. Remote Sens. 2013; 5: 5265–5284.

39. Clevers JGPW, Kooistra L, Schaepman ME. Estimating canopy water content using hyperspectral remote sensing data. Int J Appl Earth Obs Geoinf. 2010; 12: 119–125.

40. Vohland M. Using imaging and non-imaging spectroradiometer data for the remote detection of vegetation water content. J Appl Remote Sens. 2008; 2: 023520.

41. Penuelas J, Filella I, Serrano L, SavÉ R. Cell wall elasticity and Water Index (R970 nm/R900 nm) in wheat under different nitrogen availabilities. Int J Remote Sens. 1996; 17: 373–382.

42. Zarco-Tejada PJ, Rueda CA, Ustin SL. Water content estimation in vegetation with MODIS reflectance data and model inversion methods. Remote Sens Environ. 2003; 85: 109–124.

43. Hunt ER, Rock BN. Detection of changes in leaf water content using near- and middle-infrared reflectances. Remote Sens Environ. 1989; 30: 43–54.

44. Hardisky M, Klemas V, Smart R. The influence of soil-salinity, growth form, and leaf moisture on the spectral radiance of spartina-alterniflora canopies. Photogramm Eng Remote Sens. 1984; 49: 77–83.

45. Ceccato P, Flasse S, Grégoire JM. Designing a spectral index to estimate vegetation water content from remote sensing data. Remote Sens Environ. 2002; 82: 198–207.

46. Pasqualotto N, Delegido J, Van Wittenberghe S, Verrelst J, Rivera JP, Moreno J. Retrieval of canopy water content of different crop types with two new hyperspectral indices: water absorption area index and depth water index. Int J Appl Earth Obs Geoinf. 2018; 67: 69–78.

47. Danson FM, Bowyer P. Estimating live fuel moisture content from remotely sensed reflectance. Remote Sens Environ. 2004; 92: 309–321.

48. Zhao CJ, Zhou Q, Wang J, Huang WJ. Band selection for analysing wheat water status under field conditions using relative depth indices (RDI). Int J Remote Sens. 2010; 25: 2575–2584.

49. Wang JN, Zheng LF, Tong QX. The spectral absorption identification model and mineral mapping by imaging spectrometer Data. Remote Sens Environ China. 1996; 11: 20–31.

50. Ma J, Sun DW, Pu H. Spectral absorption index in hyperspectral image analysis for predicting moisture contents in pork longissimus dorsi muscles. Food Chem. 2016; 197: 848–854. https://doi.org/10.1016/j.foodchem.2015.11.023 PMID: 26617026

51. Li Z, Guo XD, Gi C, Zhao J. A new vegetation index infusing visible-infrared spectral absorption feature for natural grassland FAPAR retrieval. Guang Pu Xue Yu Guang Pu Fen Xi. 2017; 37: 859–864. PMID: 30160401

52. Verrelst J, Rivera JP, Veroustraete F, Muñoz-Marí J, Clevers JGPW, Camps-Valls G, et al. Experimental sentinel-2 LAI estimation using parametric, non-parametric and physical retrieval methods–A comparison. ISPRS J Photogramm Remote Sens. 2015; 108: 260–272.

53. Kawamura K, Watanabe N, Sakanoue S, Inoue Y. Estimating forage biomass and quality in a mixed sown pasture based on partial least squares regression with waveband selection. Grassl Sci. 2008; 54: 131–145.

54. Ceccato P, Gobron N, Flasse S, Pinty B, Tarantola S. Designing a spectral index to estimate vegetation water content from remote sensing data: part 1. Remote Sens Environ. 2002; 82: 188–197.